Journal of Applied Polymer Science

Adsorption of Hg(II) in Aqueous Solutions Using Mercapto-Functionalized Alkali Lignin

Yan Zhou,[1] Jianping Zhang,[2,3] Xuegang Luo,[2] Xiaoyan Lin[2]

[1]College of Chemistry and Chemical Engineering, Mianyang Normal University, Mianyang 621000, Sichuan, China

[2]Engineering Research Center of Biomass Materials, Ministry of Education, Southwest University of Science and Technology, Mianyang 621010, Sichuan, China

[3]The Eighth Research Institute, China Academy of Engineering Physics, Mianyang 621900, Sichuan, China

Correspondence to: Y. Zhou (E-mail: zjpzy@126.com)

ABSTRACT: A novel adsorbent for Hg(II), mercapto-functionalized alkali lignin (AL-SH) was synthesized by Friedel–Crafts alkylation reaction and nucleophilic substitution reactions. The adsorbent was characterized by the techniques of Fourier transform-infrared spectroscopy (FT-IR), elementary analysis and thermogravimetric analysis, and N_2 adsorption techniques. The effect of various parameters on Hg(II) adsorption process such as initial pH, contact time, ionic strength, initial Hg(II) concentration, temperature, and adsorbent dosage were investigated in detail through batch static experiments. The results indicated that the adsorption process of Hg(II) on AL-SH was mainly dependent on the pH and the optimal pH value was at pH ranging from 4.0 to 6.0. The adsorption process was found to follow pseudosecond-order kinetics and the main process was chemical adsorption, which equilibrated at 8 h. The adsorption isotherm was better described by Langmuir and Temkin isotherm equations compared to Freundlich isotherm equation and the maximum adsorption capacity obtained was 101.2 mg g^{-1} (pH = 4.0, 20°C, initial Hg(II) concentration was 200 mg L^{-1}). The thermodynamic parameters of ΔH^0_{ad} and ΔS^0_{ad} were positive while ΔG^0_{ad} was negative, revealed that the adsorption of Hg(II) onto AL-SH was a spontaneous and endothermic process with increased entropy. © 2014 Wiley Periodicals, Inc. J. Appl. Polym. Sci. **2014**, *131*, 40749

KEYWORDS: adsorption; functionalization of polymers; kinetics; separation techniques

Received 12 October 2013; accepted 22 March 2014

DOI: 10.1002/app.40749

INTRODUCTION

Mercury is widely used in the chlor-alkali, plastics, metallurgy, electronics, and other industries because of its unique properties.[1] However, the Hg(II)-containing wastewater discharged from these industries has created a major global concern due to its bioaccumulative and its potential risk to human health.[2] Hence, controlling of mercury emissions has been recognized to be extremely important to the environment and biota. In recent years, much effort has been devoted to developing techniques to remove Hg(II) from water such as chemical precipitation, ion exchange, membrane filtration, electrolytic methods, solvent extraction, reverse osmosis, and adsorption.[3–14] Among the methods mentioned above, adsorption technique using low-cost biosorbents is an attractive and economical one for the treatment of Hg(II)-laden wastewater owing to its easiness of operation and simplicity of design. Therefore, it is especially important to develop a low-cost adsorbent with strong affinities and high uptake capacity, such as lignin, chitosan, agricultural byproducts, and polysaccharide materials to adsorb the targeted heavy metal ions from wastewater.[15–18]

Lignin, next to cellulose, is an abundant and renewable biomaterial widespread in every vascular plant. The structure is composed of three different types of phenylpropane units, which linked together with ether and carbon–carbon linkages formed an irregular three-dimensional network biopolymer.[19] Alkali lignin is generally produced mainly coming from pulp and paper making industry and biomass fractionation. The molecule contains many active functional groups such as hydroxy, phenol hydroxy, carboxyl, and methoxy group, which make lignin as a promising material for ion exchange and adsorption.[20] However, the relatively poor capacity of alkali lignin limits its applications as an adsorption material to remove heavy metals. Consequently, it is necessary to introduce functional group(s) with high affinity and selectivity for specified metal ions to prepare some advanced lignin adsorbent through chemical modification reaction. Mercapto groups strongly bonded with mercury compounds have shown high affinity and high selectivity for Hg(II) removal from aqueous media.[21–24]

In our previous study, chlorinated lignin (ChL) was prepared successfully after treating alkali lignin with 1,2-dichloroethane

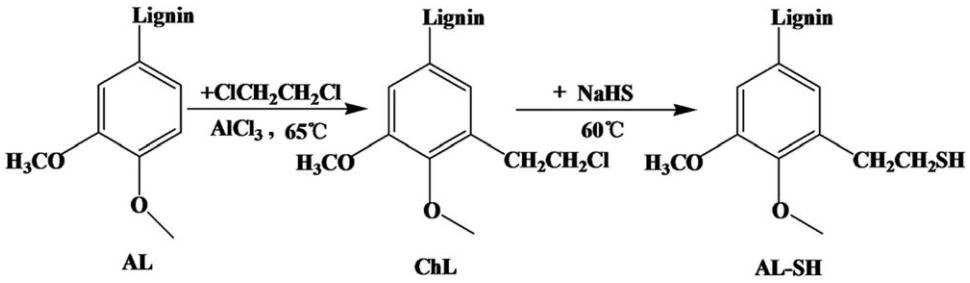

Scheme 1. Synthesis route of AL-SH.

(DCE) by Friedel–Crafts alkylation reaction and then the ChL was modified via nucleophilic substitution with ethylenediamine to increase its functionality and surface activity.[25] Based on the previous study, we prepared a novel mercapto-functionalized ChL and used it to remove Hg(II) ions from aqueous solutions. The characterization of adsorbent was analyzed by fourier transform-infrared spectroscopy (FT-IR), element analysis, thermogravimetric analysis (TGA), and N_2 adsorption techniques. The effects of experimental parameters such as pH, ionic strength, contact time, initial concentration, temperature, and adsorbent dosage on adsorption were also investigated in batch systems.

EXPERIMENTAL

Materials

Alkali lignin was purchased from Shandong Yiyuan Xuemei Paper Company (Shangdong, China) and was used without further purification. 5-Br-PADAP (98%) was obtained from Aladdin Chemical. DCE, anhydrous aluminum chloride, Mercury(II) chloride, and other chemicals used in this work were analytical grade and obtained from Kelong Chemicals Company (Chengdu, China). NaHS solution (30%, mass fraction) was synthesized in the laboratory.

Preparation of Modified Alkali Lignin

Preparation of ChL. ChL was prepared according to the method described in our previous work. Briefly, 20 g of alkali lignin and 250 mL of DCE were catalyzed by 60 g of anhydrous aluminum chloride, maintaining the reaction temperature at 65°C for 6 h with magnetic stirring. The reaction was quenched by adding mixture of ice water followed by dilute hydrochloric acid. The products (ChL) were thoroughly washed with distilled water and then with acetone and finally dried overnight at 90°C for further preparation.

Preparation of Mercapto-Functionalized Alkali Lignin (AL-SH). Twenty five grams of ChL and 200 mL NaHS aqueous solution were added into a three-necked round-bottomed flask with magnetic stirring. After stirring overnight at room temperature, the reactor was immersed into a water bath at 60°C and refluxed while stirring for 4 h, then the mixture was acidified with HCl. The precipitate was filtered out and washed with distilled water thoroughly till no precipitate could be detected in filtrate by 0.1 mol L^{-1} $AgNO_3$ solution. The AL-SH product was dried in a convection oven at 80°C for 24 h. The total preparation processes of AL-SH are expressed in Scheme 1.

Characterization

FT-IR spectra of dried samples in potassium bromide discs were recorded at 400–4000 cm^{-1} using a Nicolet-5700 model FT-IR spectrometer. Elemental analysis of AL and AL-SH were carried out with a Vario EL cube elemental analysis instrument. The thermogravimetric analysis (TGA) were performed with a Mettler SDTA851^e instrument system at a heating rate of 20°C min^{-1} up to 900°C in N_2 atmosphere. Specific surface areas, pore volumes, and pore radius' of samples were determined with N_2 adsorption at a liquid nitrogen temperature (77 K) on a surface analyzer (SSA-4200, Beijing Builder Electronic Technology Co.). Prior to analysis, the samples were degassed for 12 h at 130°C in a vacuum system at a pressure lower than 10^{-4} Torr. The specific surface area of the sample was calculated by the BET method, and the total pore volume was evaluated from the last point of the isotherm at relative pressure equal to 0.998.

Sorption Experiments

The samples of AL-SH used for Hg(II) adsorption were investigated at different initial pH, ionic strength, contact time, initial concentration of Hg(II), temperature, and adsorbent dosage. The Hg^{2+} stock solution (500 mg L^{-1}) was prepared by dissolving $HgCl_2$ in double-distilled water and acidified with concentrated HCl to prevent hydrolysis. The desired different initial concentration of Hg(II) was prepared by proper dilution of the stock solution. The initial pH of the Hg(II) solution was adjusted to the desired pH by sodium hydroxide (0.1 mol L^{-1}) and hydrochloric acid (0.1 mol L^{-1}). The ionic strength of the solution was adjusted by KNO_3. All adsorption experiments were carried out in triplicate by shaking a fixed amount of AL-SH with 100 mL of Hg(II) ions aqueous solution at a predetermined concentration, desired pH, ionic strength, and temperature in an electrically thermostatic reciprocating shaker at 150 rpm and mean value of the results (differences less than 3%) were used for data analysis. After adsorption, solid–liquid separation was achieved by centrifugation at 5000 rpm for 10 min, and the residual Hg(II) concentrations were analyzed by 5-Br-PADAP spectrophotometric method at 563 nm.[26] (To make

Table I. Elemental Analysis of AL-SH and AL

	Element/%(mass)			
Sample	C	H	N	S
AL-SH	59.51	5.124	0.53	5.276
AL	59.74	5.386	0.94	1.273

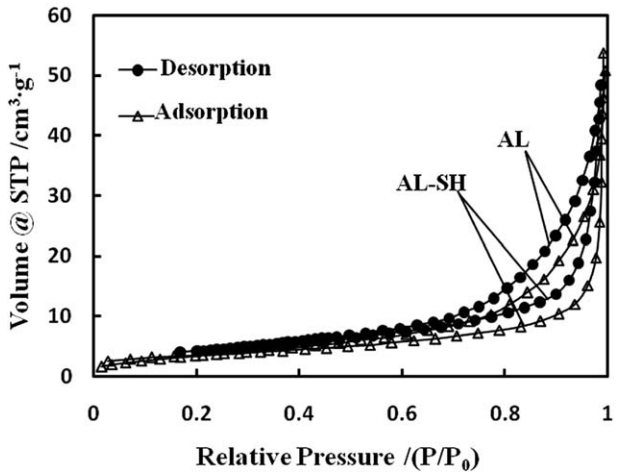

Figure 1. Nitrogen adsorption–desorption isotherms of AL and AL-SH.

Table II. Pore structure Parameters of AL-SH and AL

Sample	BET (m^2 g^{-1})	Total pore volume (cm^3 g^{-1})	Mean pore diameter (nm)
AL-SH	11.72	0.083	14.26
AL	12.98	0.079	12.17

spectrophotometric determination, 5 mL of the sample solution containing not more than 35 μg of mercury was transferred to a 25 mL volumetric flask, then 1.5 mL of 5-Br-PADAP which was prepared by dissolution in ethanol (0.5 mmol L^{-1}), 3 mL of borax-hydrochloric acid buffer solution (pH 9.10), and 3 mL of sodium dodecyl sulfate (10 g L^{-1}) were successively added. Finally, the mixture was diluted to the mark with distilled water and shaken properly to get it well mixed, then set aside for 5 min and measured the absorbance at 563 nm against a reagent blank. A calibration curve was prepared for 0–35 μg of mercury). All the experimental data were the average of triplicate determinations, and the average uncertainties were <5%. The equilibrium adsorption capacity q_e (mg g^{-1}) and removal efficiency (E%) was calculated as follows:

$$q_e = \frac{(C_0 - C_e)V}{1000w} \quad (1)$$

$$E(\%) = \frac{C_0 - C_e}{C_0} \times 100 \quad (2)$$

where C_0 (mg L^{-1}) and C_e (mg L^{-1}) are the initial Hg(II) concentration and Hg(II) concentration after adsorption, respectively. V is the volume of the solution in mL and w is the weight of the adsorbent in g.

RESULTS AND DISCUSSION

Characterization

On comparison between the FT-IR spectrum of alkali lignin and that of the AL-SH (figure not shown here), it was found that within a certain scope, the characteristic groups of AL-SH are almost the same to those of AL, their spectra are similar to each other, just the peak intensities changes. The appearance of new double peaks of S–H were found at 2338 and 2362 cm^{-1}, which are typically very weak due to the aggregation of mercapto groups within the monolayer and hydrogen binding effects.[27] The results demonstrated that the modification on AL not only introducing new functional groups (—SH) successfully but also remain the primary functional groups of AL.

The elemental analyses (C, H, N, and S) of dried samples of AL and AL-SH are given in Table I. The results indicated that the elements C, H, N, and S were present both in the AL and AL-SH samples. The C, H, and N contents of AL-SH were slight declined than those of AL, which were ascribed the increase of total mass after chemical modification. Whereas the sulfur contents of AL-SH were 4% richer than that of AL. The above results implied that —SH fractions were introduced onto AL successfully.

In general, it was thought that large specific surface areas and pore volumes was attributed to better physical adsorption.[28–30] Figure 1 shows the nitrogen adsorption–desorption isotherm and pore size distribution of alkali lignin and AL-SH, and the pore characteristics are shown in Table II Compared with

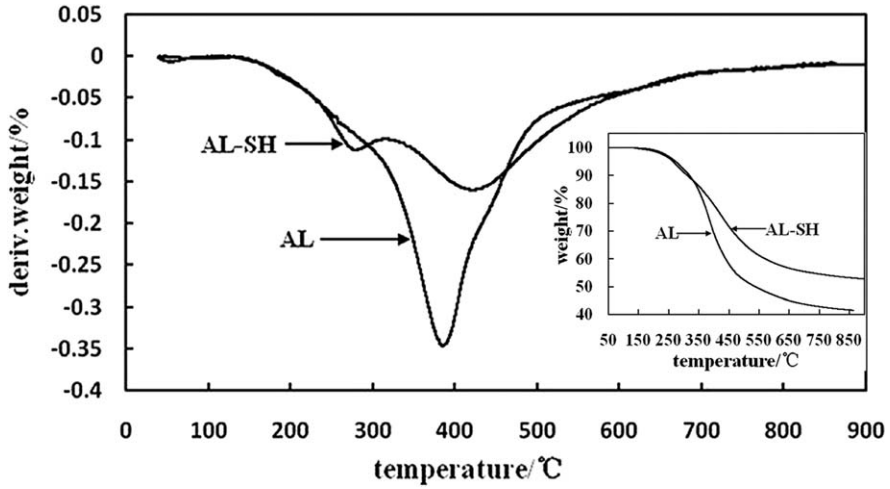

Figure 2. DTG and TG curves of AL and AL-SH.

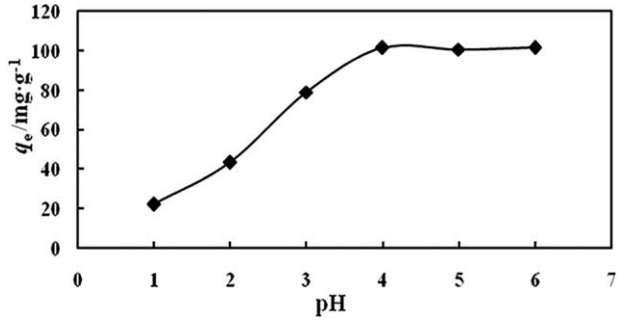

Figure 3. Effect of pH on adsorption of Hg(II) (Hg(II): 200 mg L^{-1}, adsorbent dose: 1 g L^{-1}, contact time: 12 h and temperature: 20°C).

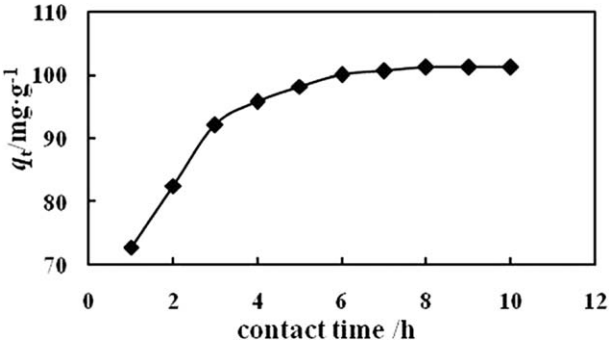

Figure 5. Effect of contact time on adsorption of Hg(II) on AL-SH (Hg(II): 200 mg L^{-1}, adsorbent dose: 1 g L^{-1}, pH: 4.0 and temperature: 20°C).

alkali lignin, the BET surface areas of AL-SH became lower after chemical modification. It might suggest that some large pores became clogged after chloration and sulfhydrylation. However, the introduced mercaptoethyl groups could bring excellent effects on the pore enlargement, therefore, the total pore volume and pore diameter increased, which benefit to expose the active sites and also benefit to chemical sorption. It can be concluded that mercapto-functionalized AL presents an adequate physical and chemical characteristics to adsorb metal ions. These findings were parallel to the Smaail Radi's work.[31]

Thermogravimetric curves of virgin lignin and AL-SH were investigated (Figure 2) and the DTG curve of the alkali lignin exhibited a relatively simple band with a peak at around 384°C, indicating an almost single decomposition stage. Whereas AL-SH exhibited a significant two-stage decomposition band. The peak at 279°C may be attributed to the breakage of functionalized groups of AL-SH as a result of degassing hydrogen sulfide. The second peak at 420°C corresponds to the decomposition of the modified lignin backbone. For a main decomposition temperature shifting higher from AL to AL-SH it indicated that —SH grafting to the lignin structure would help to improve the thermal stability of modified alkali lignin since the AL-SH has about 40°C higher thermal decomposition temperature compared to that of raw alkali lignin. A reasonable explanation that can be considered is that of an interchain steric hindrance caused by chlorination process, Friedel–Crafts alkylation reaction, and nucleophilic substitution reactions, which impeded the chemical bond breakage. All analysis results indicate the reactions shown in Scheme 1 are carried out as expected.

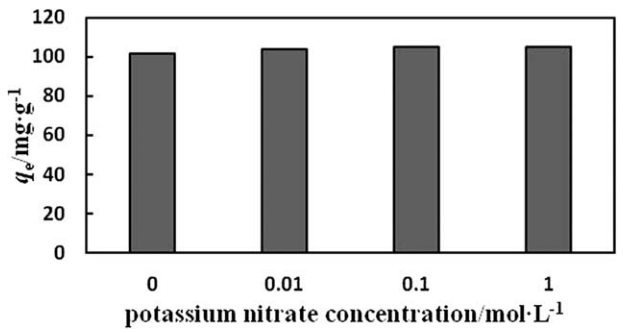

Figure 4. Effect of ionic strength on Hg(II) adsorption of AL-SH (initial Hg(II): 200 mg L^{-1}, adsorbent dose: 1 g L^{-1}, pH = 4.0, contact time: 12 h and temperature: 20°C).

Adsorption of Hg(II) on AL-SH

Effect of pH on Adsorption. Aqueous phase pH is one of the most important factors on metal ion adsorption onto adsorbent, which affect the dissociation of active functional sites on the sorbent and also governs the hydrolysis, complexation, and precipitation of metals.[32] The effect of pH value on the adsorption amount of AL-SH is given in Figure 3. As it is shown, the pH increasing from 1.0 to 4.0, the adsorption capacity of Hg(II) ions increases with the optimum achieved at pH 4.0 and remains nearly constant up to pH 6.0. At this pH range (4.0–6.0), Hg(II) ions exist as Hg^{2+} and $HgCl^{+}$ species in water solution. With the introduction of mercapto groups (—SH) onto the AL, Hg(II) ions could be absorbed by AL-SH to form stable AL-S-Hg-S-AL and AL-S-HgCl complex.[17,33] It is known that mercapto group (—SH) is a weak acid chelate group and has great affinity for H^{+}. The AL-S-Hg-S-AL and AL-S-HgCl complex become instable when the pH decreased, the adsorption capacity of Hg(II) ions thereupon decreased. At higher pH values (>6.0), precipitation of Hg(II) hydroxide occurs simultaneously with the adsorption of Hg(II) ions.[34] Hence, pH = 4.0 was chosen for the adsorption of Hg(II) ions.

Effect of Ionic Strength on Adsorption. Extensive investigations carried out on adsorption of Hg(II) revealed that the adsorption capacity of Hg(II) was strongly influenced by the concentration of the electrolyte ion added to the solution and found that a rise in ionic strength led to a decrease in the Hg(II) uptake capacity because of the decrease in the activity of metal ions and the increase in concentration of competing cations.[35–37] Figure 4 presents the effect of the ionic strength on the Hg(II) adsorption capacity. As seen in Figure 4, increasing the ionic strength from 0 to 1 mol L^{-1} did not lead to a decrease in Hg(II) adsorption. It is noteworthy that inorganic salt has not shown significant interference in Hg(II) uptake. The adsorption capacity of Hg(II) on AL-SH remains almost constant, which may be further specified that the mercapto groups of AL-SH mainly contributed to metal uptake. Similar results happened to Hg(II) adsorption on amine-modified attapulgite37 and polyaniline/attapulgite composite.[38] Considering the ineffective of ionic strength on the Hg(II) adsorption

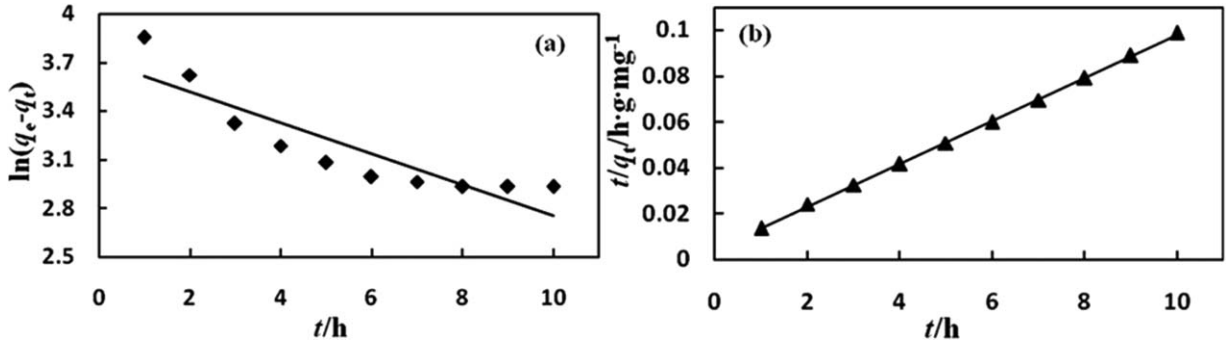

Figure 6. The pseudofirst-order kinetics (a) and the pseudosecond-order kinetics (b) for the adsorption of Hg(II) onto AL-SH.

capacity, the ionic strength was not adjusted in the following experiments.

Effect of Contact Time and Adsorption Kinetics. The effect of contact time on the adsorption extent of Hg(II) on AL-SH (Figure 5) was investigated at initial Hg(II) concentration of 200 mg L^{-1} using 1 g L^{-1} of adsorbent dosage (pH = 4.0, 20°C). Figure 5 shows that a rapid initial uptake rate of Hg(II) in the first 3 h and, thereafter, the adsorption rate slowly declined with lapse of contact time and it remained practically constant after adsorption equilibrium was established at about 8 h. The variation in the extent of adsorption may be due to the fact that numerous vacant surface sites were available for adsorption during the initial stage and the solute concentration gradient was relatively high. Consequently, the extent of Hg(II) species removal decreased with the increase of contact time, which was dependent on the decrease in the availed adsorption site on the surface of AL-SH and the decreased Hg(II) solute concentration gradient, and also the repulsive forces between Hg(II) ions adsorbed on the AL-SH and the solution phase.[39] Generally, when adsorption involves a surface reaction process, the initial adsorption is rapid and as the availed adsorption site gradually decreases, the lower adsorption rate would follow. This is consistent with studies reported before.[40,41] Considering the sufficient removal of Hg(II) by AL-SH, the contact time was set to 8 h in the following experiments to ensure adsorption conditions were achieved.

According to the data obtained from this experiment, different kinetic models including pseudofirst-order, pseudosecond-order model, and intraparticle diffusion models have been used to explicate the potential rate-controlling steps and predict the adsorption kinetics of the adsorption process. The Lagergren pseudofirst-order model and pseudosecond-order kinetic model were expressed by the following eqs. (3) and (4), respectively.[42,43]

$$\ln(q_e - q_t) = \ln q_e - k_1 t \tag{3}$$

$$\frac{t}{q_t} = \frac{1}{k_2 q_e^2} + \frac{t}{q_e} \tag{4}$$

where t is the contact time (h), q_t and q_e are the amounts of Hg(II) absorbed at time t and at equilibrium (mg g^{-1}), respectively. k_1 (h^{-1}) and k_2 (g(mg h)$^{-1}$) is the rate constant of pseudofirst-order and pseudosecond-order adsorption, respectively. Plotting ln ($q_e - q_t$) and t/q_t against t (Figure 6) enables one to obtain k_1, k_2, and $q_{e(cal)}$ from the slope and intercept, and the results are listed in Table III. As it is evident in Table III, the calculated equilibrium adsorption capacity $q_{e(cal)}$ using the pseudosecond-order model is much closer to the experimental $q_{e(exp)}$ values, other than the dramatic difference between $q_{e(exp)}$ and $q_{e(cal)}$ from pseudofirst-order model, the R^2 value of pseudosecond-order kinetics model is higher than that of pseudofirst-order kinetics model. So, it can be concluded that the adsorption kinetics of Hg(II) on AL-SH fit better into the pseudosecond-order kinetics model in contrast to the pseudofirst-order model. The pseudosecond-order rate law expression is based on the assumption that the rate limiting step is chemical sorption.[44] It is possible to say that the Hg(II) ions adsorbed on mercapto groups grafted in AL-SH via chemical sorption or chemisorptions. Similar results have been obtained for Hg(II) adsorption by polyacrylamide/attapulgite,[45] thiourea-modified magnetic chitosan microspheres,[46] and formaldehyde crosslinked-modified chitosan–thioglyceraldehyde Schiff's base.[47]

The kinetic experimental data were also applied to the intraparticle diffusion model using the following equation.[48]

$$q_t = k_i t^{\frac{1}{2}} + C \tag{5}$$

where q_t (mg g^{-1}) is adsorption capacity at any time t, k_i (mg $h^{1/2}$ g^{-1}) is the intraparticle diffusion rate constant and C (mg g^{-1}) is the film thickness. If intraparticle diffusion is the rate-limiting step, the plot of q_t against $t^{1/2}$ should be a straight line and pass through the origin. In contrast, if the experimental

Table III. The Kinetics Parameters for the Adsorption of Hg(II) on AL-SH

	Pseudofirst-order			Pseudosecond-order		
$q_{e(exp)}$ (mg g^{-1})	k_1 (h^{-1})	$q_{e(cal)}$ (mg g^{-1})	R^2	k_2 (g mg^{-1} h^{-1})	$q_{e(cal)}$ (mg g^{-1})	R^2
101.2	0.09	40.9	0.804	0.02	111.1	0.999

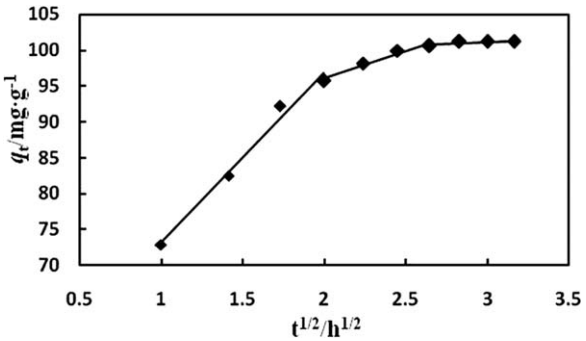

Figure 7. Intraparticle diffusion model for the adsorption of Hg(II) on AL-SH.

data exhibit multilinear plots, two or more steps influence the adsorption process.[49] Figure 7 shows the plot of the amount of Hg(II) adsorbed (q_t) versus the square root of time ($t^{1/2}$). It is evident from Figure 7 that the intraparticle diffusion plot in this case was not through the origin and can distinguish three distinct regions. The sharp first linear portion is attributed to the film diffusion and the second linear portion is due to the pore diffusion. The third portion indicates the final equilibrium stage where intraparticle diffusion starts to slow down because of the extremely low adsorbate concentrations in the solution.[50,51] This suggests that the adsorption of Hg(II) on AL-SH involved intraparticle diffusion, but it was not the only rate-controlling step.

Effect of Initial Concentration and Isotherm Model. The effect of the initial Hg(II) concentration on the adsorption capacity and the adsorption isotherms of Hg(II) on AL-SH are displayed in Figure 8. Experimental studies were carried out with varying the initial Hg(II) concentration from 50 to 300 mg L^{-1} at 20°C, using 1 g L^{-1} of adsorbent dosage at pH 4.0 for 8 h. As can be seen from Figure 8, the equilibrium adsorption amount increased significantly along with increasing initial concentration; this meant that the adsorption process was highly concentration dependent. The increase in the adsorption capacity of AL-SH with relation to Hg(II) concentration was probably due to the saturation of available active adsorption sites on AL-SH and a high driving force for mass transfer. Similar results were reported in metal ions adsorption by other researchers.[52–55]

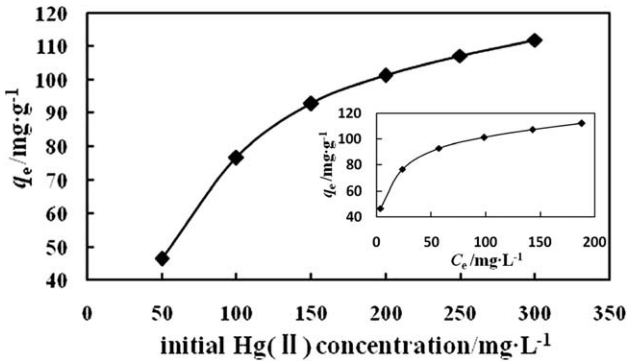

Figure 8. Effect of Hg(II) concentration and adsorption isotherms of Hg(II) on AL-SH (contact time: 8 h, adsorbent dose: 1 g L^{-1}, pH: 4.0 and temperature: 20°C).

However, above a certain concentration, there was a slow increase in the adsorption capacity, which tended toward saturated values with a decrease in the content of available mercapto groups. For an initial Hg(II) concentration of the 300 mg L^{-1}, the saturation adsorption capacities of Hg(II) on AL-SH were found to be 112 mg g^{-1}.

The equilibrium data for this study were analyzed in the light of three well-known models: Langmuir, Freundlich, and Temkin models. The Freundlich isotherm assumes nonideal sorption on heterogeneous surfaces and multilayer sorption, Langmuir isotherm is used for the monolayer adsorption on a homogenous surface, whereas Temkin isotherm suggests that the heat of adsorption would decrease linearly with the increase of the coverage of the sorptional centers of an adsorbent. The adsorption equilibrium data presented in Figure 8 were applied to Langmuir isotherms eq. (6), Freundlich isotherms eq. (7), and Temkin isotherm eq. (8).[12] Their expressions can be presented by the following equations:

$$\frac{C_e}{q_e} = \frac{C_e}{q_{\max}} + \frac{1}{q_{\max} b} \tag{6}$$

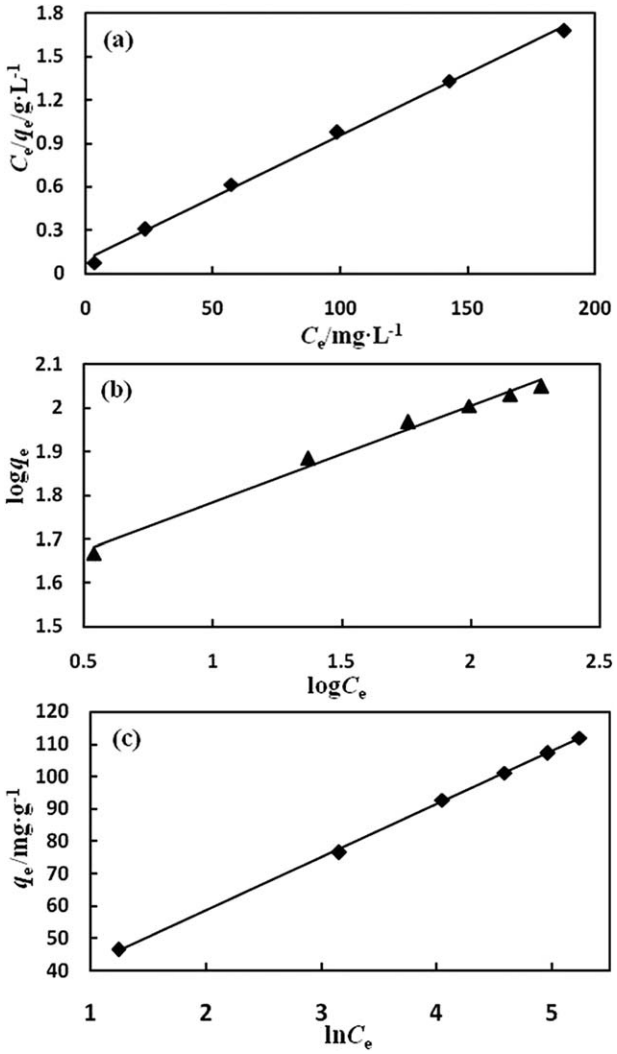

Figure 9. Langmuir (a), Freundlich (b), and Temkin (c) isotherm model for the Hg(II) adsorption onto AL-SH.

Table IV. Isotherm Parameters for the Adsorption of Hg(II) by AL-SH

Langmuir equation			Freundlich equation			Temkin equation		
b (L mg^{-1})	q_{max} (mg g^{-1})	R^2	n	K_F (mg g^{-1})(mg L)$^{1/n}$	R^2	A (L g^{-1})	B	R^2
0.086	125	0.997	4.55	36.56	0.988	4.80	16.43	0.999

Table V. Maximum Uptake Capacity for the Adsorption of Hg(II) onto Various Biosorbents

Biosorbent	Temperature (°C)	q_{max} (mg g^{-1})	Reference
AL-SH	20	125	Present work
Lignin	24 ± 1	74.7	[17]
Ethylenediamine modified peanut shells	25	30.72	[30]
Formaldehyde crosslinked modified chitosan-thioglyceraldehyde Schiff's base	30	98 ± 2	[47]
Rice husk ash	15	9.32	[58]
Crosslinked chitosan membranes	25	75.5	[59]
Chemically modified Egyptian mandarin peel	20	23.26	[12]
Malt spent rootlets	25	50.4	[60]
Lichen (*Xanthoparmelia conspersa*)	20	82.8	[61]

$$\log q_e = \log K_F + \frac{1}{n}\log C_e \quad (7)$$

$$q_e = B \ln A + B \ln C_e \quad (8)$$

where q_e(mg g^{-1}) and C_e(mg L^{-1}) are the amount of adsorbed Hg(II) per unit weight of adsorbent and Hg(II) concentration in solution at equilibrium, respectively. K_F ((mg g^{-1})(mg L)$^{1/n}$) indicates the multilayer adsorption capacity and n, an empirical parameter related to the intensity of adsorption. b (L mg^{-1}) is Langmuir constant relating the free energy of adsorption. q_{max} (mg g^{-1}) is the monolayer uptake capacity of the adsorbent. A and B are the Temkin constants, A is the equilibrium binding constant corresponding to the maximum binding energy and constant B is related to the heat of adsorption.[56] The Langmuir, Freundlich, and Temkin constants were calculated from the slopes and intercepts of the plots of C_e/q_e versus C_e [Figure 9(a)], log q_e versus log C_e [Figure 9(b)], and q_e versus ln C_e [Figure 9(c)] and were represented in Table IV. The Freundlich constant value of n obtained is 4.55 and K_F is 36.56 ((mg g^{-1})(mg L)$^{1/4.55}$) indicating that the adsorption was favorable. From the Langmuir isotherm, the predicted maximum adsorption capacities ($q_{max(cal)}$) is 125 mg g^{-1}, which is very close to the experimental value. By comparing the correlation coefficients, it can be concluded that the Langmuir and Temkin equation in which R^2 are close to unity to fit the experimental data better than the Freundlich isotherm equation for the description of the adsorption equilibrium system. Therefore, it could be stated that the adsorption of Hg(II) onto AL-SH generates in both monolayer sorption and heterogeneous surface conditions as the high values of the correlation coefficient between the adsorbate–adsorbent system for the three isotherm models.[57] A comparison of the maximum adsorption capacities ($q_{max,(cal)}$) for Hg(II) ions obtained in this work with some other biosorbents for Hg(II) reported in the literature from the Langmuir model is shown in Table V.

Effect of Temperature and Adsorption Thermodynamics. To investigate the effect of the temperature (20, 30, 40, 50, and 60°C) on the Hg(II) adsorption, the experiments were conducted at constant initial concentrations of Hg(II) (200 mg L^{-1}), pH of 4.0 for 8 h. The results are shown in Figure 10. As can be seen from Figure 10, temperature has great influence on the adsorption capacity. The adsorption capacity of AL-SH for Hg(II) almost linear increases with the increasing of temperature. The thermodynamic parameters such as standard Gibbs free energy of adsorption (ΔG^0_{ad}), enthalpy change (ΔH^0_{ad}), and entropy change (ΔS^0_{ad}) were calculated using the following equations:

$$\Delta G^0_{ad} = -RT \ln K_{ad} \quad (9)$$

$$\ln K_{ad} = \frac{\Delta H^0_{ad}}{RT} + \frac{\Delta S^0_{ad}}{R} \quad (10)$$

where K_{ad} is the thermodynamic equilibrium constant defined by $K_{ad} = q_e/C_e$, R is the ideal gas constant, and T is the absolute temperature (K). By plotting ln K_{ad} versus T^{-1} (shown in

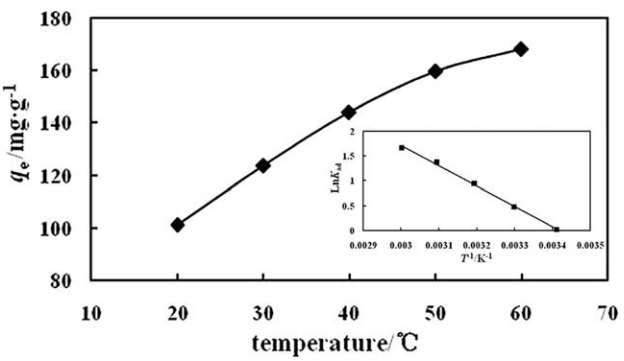

Figure 10. Effect of temperature and the relationship of ln K_{ad} and T^{-1} (Hg(II): 200 mg L^{-1}, adsorbent dose: 1 g L^{-1}, pH: 4.0 and contact time: 8 h).

Table VI. Thermodynamic Parameters of Hg(II) Adsorption on AL-SH

T (°C)	K_{ad}	ΔG^0_{ad} (kJ mol^{-1})	ΔH^0_{ad} (kJ mol^{-1})	ΔS^0_{ad} J·(mol K)$^{-1}$	R^2
20	1.025	−0.059			
30	1.615	−1.208			
40	2.573	−2.459	33.97	116.1	0.997
50	3.963	−3.698			
60	5.278	−4.467			

Figure 10), the values of ΔH^0_{ad} and ΔS^0_{ad} can be calculated from the slope and intercept, and they are given in Table VI. As is evident in Table VI, ΔG^0_{ad} is negative sign at the defined temperature, which suggests the spontaneous nature of Hg(II) adsorption onto the AL-SH. In addition, with the increasing of temperature, ΔG^0_{ad} decreases, which reveals that the sorption process of Hg(II) on AL-SH is more favorable at higher temperatures. This is in good agreement with their adsorption capacities. The positive values of ΔH^0_{ad} indicate that the adsorption of Hg(II) on the AL-SH is an endothermic process. In addition, the positive value of ΔS^0_{ad} suggests the increasing randomness at the solid/solution interface during the adsorption and indicates the stability of adsorption process with no structural change at solid–liquid interface.[62,63]

Effect of Adsorbent Dosage. The adsorbent dosage is an important parameter because it determines the removal ability of an adsorbate. The effect of AL-SH dosage on the Hg(II) adsorption process was studied at temperature 20°C with varying amounts (0–5 g L^{-1}) of AL-SH using 100 mL of initial concentration of Hg(II) at 200 mg L^{-1} at pH 4.0 and the results are illustrated in Figure 11. It can be seen that the removal efficiency increases with increasing AL-SH dosage, which could be attributed to the more available active sites and the higher surface area for adsorption. With the AL-SH dosage increasing to approximate 4 g L^{-1}, the removal efficiency approaches to 90% and then increases slightly with AL-SH dosage. The maximum removal efficiency is over 94% when AL-SH dosage reaches 5 g L^{-1}. Conversely, the adsorption capacity (q_e) decreases with increasing the AL-SH dose. The

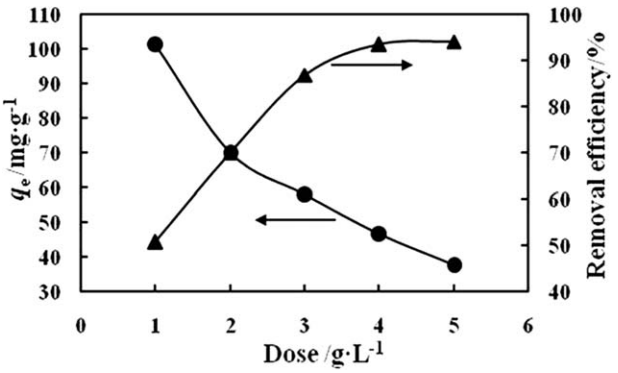

Figure 11. Effect of AL-SH dosage on removal of Hg(II) from aqueous solution. (Hg(II): 200 mg L^{-1}; pH 4.0; temperature: 20°C and contact time: 8 h).

observed decrease in adsorption capacity is due to adsorption sites remaining unsaturated during the adsorption process.

CONCLUSIONS

Based on the experimental results, the following conclusions are made.

1. A novel mercapto-modified alkali lignin (AL-SH) adsorbent that has great affinity for Hg(II) was synthesized by Friedel–Crafts alkylation reaction and nucleophilic substitution reactions with alkali lignin.
2. Aqueous phase pH has great influence on the adsorption process of Hg(II) on AL-SH and the optimal pH value was at pH ranging from 4.0 to 6.0. To some degree, the adsorption capacities depend partly on the contact time, and the equilibrium time was 8 h, the result of fitted adsorption kinetics curve indicated that the adsorption process fit better into the pseudosecond-order kinetics model.
3. The adsorption isotherm model of AL-SH for Hg(II) was better described by Langmuir isotherm equation and Temkin isotherm equation compared to Freundlich isotherm equation.
4. The adsorption capacity of AL-SH for Hg(II) is influenced by temperature and the adsorption process was a spontaneous and endothermic process with increased entropy on the basis of thermodynamic analysis.
5. Ionic strength has not shown significant interference in Hg(II) uptake, the removal efficiency increases with increasing AL-SH dosage and the maximum removal efficiency is over 94%.

This project was financially supported by the Science and Technology Foundation of the Education Department of Sichuan Province, China (13ZB0124) and the Science and Technology Foundation of Mianyang normal university, China (2011A02)

REFERENCES

1. Wang, J. X.; Feng, X. B.; Anderson, C. W. N.; Xing, Y.; Lihai Shang, L. H. *J. Hazard. Mater.* **2012**, *221–222*, 1.
2. Li, J. R.; Mercedes Maroto-Valer, M. *Carbon* **2012**, *50*, 1913.
3. Yao, Y. X.; Velpari, V.; Economy, J. *Fuel* **2014**, *116*, 560.
4. Blue, L. Y.; Jana, P.; Atwood, D. A. *Fuel* **2010**, *89*, 1326.
5. Noh, Y. D.; Komarneni, S. *Environ. Sci. Technol.* **2011**, *45*, 6954.
6. Jaiswal, A.; Ghsoh, S. S.; Chattopadhyay, A. *Langmuir* **2012**, *28*, 15687.
7. Kim, S. G.; Hyeon, D. H.; Chun, J. H.; Chun, B. H., Kim, S. H. *J. Membr. Sci.* **2013**, *443*, 10.
8. Ozkaya, O. B.; Yigitoglu, M.; Arslan, M. *J. Appl. Polym. Sci.* **2012**, *124*, 1256.
9. Johari, K.; Saman, N.; Mat, H. *Environ. Technol.* **2014**, *35*, 629.
10. Rocha, L. S.; Lopes, C. B.; Henriques, B.; Tavares, D. S.; Borges, J. A.; Duarte, A. C.; Pereira, E. *Environ. Technol.* **2014**, *35*, 661.
11. Gupta, S.; Chakraborty, M.; Murthy, Z. V. P. *J. Dispersion Sci. Technol.* **2013**, *34*, 1733.
12. Husein, D. Z. *Desalination Water Treat.* **2013**, *51*, 6761.

13. Meeks, N. D.; Davis, E.; Jain, M.; Skandan, G.; Bhattacharyya, D. *Environ. Prog. Sustain. Energy.* **2013**, *32*, 705.
14. Zhang, S.X.; Zhang, Y. Y.; Liu, J. S.; Xu, Q.; Xiao, H. Q.; Wang, X. Y; Xu, H.; Zhou, J. *Chem. Eng. J.* **2013**, *226*, 30.
15. Wang, Z.; Yin, P.; Qu, R.; Chen, H.; Wang, C. H.; Ren, S. H. *Food Chem.* **2013**, *136*, 1508.
16. Wang, X. H.; Deng, W.; Xie, Y. Y.; Wang, C. Y. *Chem. Eng. J.* **2013**, *228*, 232.
17. Lv, J. T.; Luo, L.; Zhang, J.; Christie, P.; Zhang, S. Z. *Environ. Pollut.* **2012**, *162*, 255.
18. Nguyen, T. A. H.; Ngo, H. H.; Guo, W. S.; Zhang, J.; Liang, S.; Yue, Q. Y.; Li, Q.; Nguyen, T. V. *Bioresour. Technol.* **2013**, *148*, 574.
19. Pinkowska, H.; Wolak, P.; Złocinska, A. *Chem. Eng. J.* **2012**, *187*, 410.
20. Suteu, D.; Malutan, T.; Bilba. D. *Desalination* **2010**, *255*, 84.
21. Song, S. T.; Saman, N.; Johari, K.; Ma, H. *Ind. Eng. Chem. Res.* **2013**, *52*, 13092.
22. Li, S. Z.; Yue, X. L.; Jing, Y. M.; Bai, S. S.; Dai, Z. F. *Colloids Surf. A* **2011**, *380*, 229.
23. Wang, Y. S. ; Cheng, C. C.; Chen, J. K.; Ko, F. H.; Chang, F. C. *J. Mater. Chem. A* **2013**, *1*, 7745.
24. Standeker, S.; Veronovski, A.; Novak, Z.; Knez, Z. *Desalination* **2011**, *269*, 223.
25. Zhang, J. P.; Lin, X. Y.; Luo, X. G.; Zhang, C.; Zhu, H. *Chem. Eng. J.* **2011**, *168*, 1055.
26. Liu, Y.; Sun, X.; Li, B. *Carbohyd. Polym.* **2010**, *81*, 335.
27. Li, G. L.; Zhao, Z. S.; Liu, J. Y.; Jiang, G. B. *J. Hazard. Mater.* **2011**, *192*, 277.
28. Akkaya, B. *J. Appl. Polym. Sci.* **2013**, *130*, 2764.
29. Sarıcı-Özdemir, Ç; Önal, Y. *Desalination* **2010**, *251*, 146.
30. Li, J. G.; Feng, J. T.; Yan, W. *J. Appl. Polym. Sci.* **2013**, *128*, 3231.
31. Radi, S.; Toubi, Y.; Attayibat, A.; Bacquet, M. *J. Appl. Polym. Sci.* **2011**, *121*, 1393.
32. Li, Q. Z.; Chai, L. Y.; Qin, W. Q. *Chem. Eng. J.* **2012**, *197*, 173.
33. Pan, S. D.; Zhang, Y.; Shen, H. Y.; Hu, M.Q. *Chem. Eng. J.* **2012**, *210*, 564.
34. Monier, M.; Nawar, N.; Abdel-Latif, D. A. *J. Hazard. Mater.* **2010**, *184*, 118.
35. Singh, V.; Singh, S. K.; Maurya, S. *Chem. Eng. J.* **2010**, *160*, 129.
36. Li, R. J.; Liu, L. F.; Yang, F. L. *Chem. Eng. J.* **2013**, *229*, 460.
37. Cui, H.; Qian, Y.; Li, Q.; Wei, Z.B.; Zhai, J. P. *Appl. Clay Sci.* **2013**, *72*, 84.
38. Cui, H.; Qian, Y.; Li, Q.; Zhang, Q.; Zhai, J. P. *Chem. Eng. J.* **2012**, *211*, 216.
39. Azouaou, N.; Sadaoui, Z.; Djaafri, A.; Mokaddem, H. *J. Hazard. Mater.* **2010**, *184*, 126.
40. Xu, M.; Zhang, Y. S.; Zhang, Z.; Shen, Y.; Zhao, M. J.; Pan, G. T. *Chem. Eng. J.* **2011**, *168*, 737.
41. Chen, Y. X.; Zhong, B. H.; Fang, W. M. *J. Appl. Polym. Sci.* **2012**, *124*, 5010.
42. Lin, X. Y.; Zhang, J. P.; Luo, X. G.; Zhang, C.; Zhou, Y. *Chem. Eng. J.* **2011**, *172*, 856.
43. Xie, F.; Fan, Z. J.; Zhang, Q. L.; Luo, Z. R. *J. Appl. Polym. Sci.* **2013**, *130*, 3937.
44. Sha, B. F.; Wang, J.; Zhou, L. L.; Zhang, X. Z.; Han, L. L.; Zhao, L. *J. Appl. Polym. Sci.* **2013**, *128*, 4124.
45. Zhao, Y. J.; Chen, Y.; Li, M. S.; Zhou, S. Y.; Xue, A. L.; Xing. W. H. *J. Hazard. Mater.* **2009**, *171*, 640.
46. Zhou, L. M.; Wang, Y. P.; Liu, Z. R.; Huang, Q. W. *J. Hazard. Mater.* **2009**, *161*, 995..
47. Monier, M. *Int. J. Biol. Macromol.* **2012**, *50*, 773.
48. Li, H. M.; Huang, D. H. *J. Appl. Polym. Sci.* **2013**, *129*, 86.
49. Zhao, D. L.; Liu, C.; Liu, J. S.; Zou, J.; Li, M. *J. Appl. Polym. Sci.* **2014**, *131*, 39801.
50. Omorogie, M. O.; Babalola, J. O.; Unuabonah, E. I.; Gong, J. R. *Bioresour. Technol.* **2012**, *118*, 576.
51. Sheela, T.; Nayaka, Y. A.; Viswanatha, R.; Basavanna, S.; Venkatesha, T. G. *Powder Technol.* **2012**, *217*, 163.
52. Ghasemi, Z.; Seif, A.; Ahmadi, T. S.; Zargar, B.; Rashidi, F.; Rouzbahani, G. M. *Adv. Powder Technol.* **2012**, *23*, 148.
53. Semerjian, L. *J. Hazard. Mater.* **2010**, *73*, 236.
54. Ahmetli, G.; Yel, E.; Deveci, H.; Bravo, Y.; Bravo, Z. *J. Appl. Polym. Sci.* **2012**, *125*, 716.
55. Wang, F. Y.; Wang, H.; Ma, J. W. *J. Hazard. Mater.* **2010**, *177*, 300.
56. Bajpai, M.; Rai, N.; Bajpai, S. K. *J. Appl. Polym. Sci.* **2012**, *125*, 1382.
57. Barsanescu, A.; Buhaceanu, R.; Dulman, V. *J. Appl. Polym. Sci.* **2009**, *113*, 607.
58. Feng, Q. G.; Lin, Q. Y.; Gong, F. Z.; Sugita, S.; Shoya, M. *J. Colloid Interface Sci.* **2004**, *278*, 1.
59. Vieira, R. S.; Beppu, M. M. *Colloids Surf. A* **2006**, *279*, 196.
60. Anagnostopoulos, V. A.; Manariotis, I. D.; Karapanagioti, H. K.; Chrysikopoulos, C. V. *Chem. Eng. J.* **2012**, *213*, 135.
61. Tuzen, M.; Sari, A.; Mendil, D.; Soylak, M. *J. Hazard. Mater.* **2009**, *169*, 263.
62. Badruddoza, A. Z. M.; Tay, A. S. H.; Tan, P. Y.; Hidajat, K.; Uddin. M. S. *J. Hazard. Mater.* **2011**, *185*, 1177.
63. Kamari, A.; Ngah, W. S. W. *Colloids Surf. B* **2009**, *73*, 257.